Detailed Studies of Electron Cooling Friction Force

A.V. Fedotov[1], D. L. Bruhwiler[2], D.T. Abell[2], A.O. Sidorin[3]

[1]*Brookhaven National Lab, Upton, NY 11973*
[2]*Tech-X Corp., Boulder, CO 80303*
[3]*JINR, Dubna, Russia*

Abstract. High-energy electron cooling for RHIC presents many unique features and challenges. An accurate estimate of the cooling times requires detailed simulation of the electron cooling process. The first step towards such calculations is to have an accurate description of the cooling force. Numerical simulations are being used to explore various features of the friction force which appear due to several effects, including the anisotropy of the electron distribution in velocity space and the effect of a strong solenoidal magnetic field. These aspects are being studied in detail using the VORPAL code, which explicitly resolves close binary collisions. Results are compared with available asymptotic and empirical formulas and also, using the BETACOOL code, with direct numerical integration of less approximate expressions over the specified electron distribution function.

Keywords: electron cooling, beam dynamics, friction force
PACS: 29.28.Bd.,41.75.Lx

INTRODUCTION

The first step towards accurate calculation of cooling times is to use an accurate description of the cooling force. The achievable Coulomb logarithm in the analytic expression for the magnetized cooling force is not large. In addition, in some regimes there is a significant discrepancy between available formulas. For this reason, the VORPAL code [1] is being used to simulate from first principles the friction force and diffusion coefficients for RHIC parameters [2]. VORPAL uses molecular dynamics techniques (i.e. simulating every particle in the problem) and explicitly resolves close binary collisions to obtain the friction force and diffusion coefficient with a minimum of physical assumptions [3].

Only a few topics are addressed in this paper, but the goals of this work include the following: 1) to resolve differences in analytic formulae and semi-analytic calculations, which make assumptions such as uniform electron density, no space charge forces, infinite magnetic field, etc.; 2) to determine the validity of Z^2 scaling for friction forces, which could be broken by non-linear plasma effects in the Debye shielding for a magnetized plasma; 3) to understand the effects of bulk space charge forces; 4) to understand the effects of magnetization, from strong to weak, including magnetic field errors; 5) to accurately simulate the friction force due to magnetized collisions, in the regime of small Coulomb logarithm. In addition, for the non-magnetized concept of the RHIC cooler [4], which uses a long wiggler to focus the

CP821 *Beam Cooling and Related Topics, International Workshop on Beam Cooling and Related Topic - COOL05*
edited by S. Nagaitsev and R. J. Pasquinelli

electron beam and suppress recombination, the goals of this work include the following: 1) to explore the effects of the wiggler on the friction force, and 2) to study the effects of magnetic field imperfections. In both the magnetized and non-magnetized approaches, if the friction force for RHIC parameters deviates significantly from the description based on available formulas, it will be necessary to generate with VORPAL a table of friction coefficients for use in other codes.

The BETACOOL code has been recently enhanced [5], in order to provide benchmarking with VORPAL. In addition to the asymptotic formulas, typically used for the magnetized and non-magnetized friction force estimates, BETACOOL now includes direct numerical integration over the electron velocity distribution. This numerical evaluation of the force enables an accurate comparison with VORPAL results, both for the magnetized and non-magnetized friction force with an anisotropic velocity distribution of electrons. The results of such benchmarking are summarized in this paper.

NON-MAGNETIZED FRICTION FORCE

The friction force on an ion inside an electron beam with velocity distribution function $f(v_e)$ is described by the formula:

$$\vec{F} = -\frac{4\pi n_e e^4 Z^2 L}{m} \int \frac{\vec{v}_i - \vec{v}_e}{\left|\vec{v}_i - \vec{v}_e\right|^3} f(v_e) d^3 v_e , \tag{1}$$

where v_e and v_i are the electron and ion velocity, while L is the Coulomb logarithm:

$$L = \ln \frac{\rho_{\max}}{\rho_{\min}}, \tag{2}$$

where ρ_{max} and ρ_{min} are the maximum and minimum impact parameters, respectively. For an isotropic Maxwellian distribution of electrons, described by the function

$$f(v) d^3 v = \left(\frac{\mu}{2\pi T_e} \right)^{3/2} \exp\left(-\mu v_e^2 / 2T \right) v_e^2 dv_e d\Omega , \tag{3}$$

the friction force $\vec{F}_{NM}$ is described by the well known formula [6, 7]:

$$\vec{F}_{NM}(\vec{v}_i) = -\frac{\vec{v}_i}{v_i^3} \frac{4\pi n_e e^4 Z^2 L}{m} \varphi\left(\frac{v_i}{\Delta_e} \right), \text{ where } \varphi(x) = \sqrt{\frac{2}{\pi}} \int_0^x e^{-y^2/2} dy - \sqrt{\frac{2}{\pi}} x e^{-x^2/2}, \tag{4}$$

and Δ_e is the rms electron velocity in the rest frame of the beams (PRF), corresponding to an isotropic electron temperature $T_e = m\Delta_e^2$. Budker first suggested that this friction could be used to cool heavy ions in a storage ring [8].

The more general case of an anisotropic velocity distribution, which is the typical situation for electron cooling, can be approximated by a Maxwellian distribution with different temperatures for the longitudinal and transverse degrees of freedom:

$$f(v) d^3 v = \left(\frac{m}{2\pi} \right)^{3/2} \frac{1}{T_\perp \sqrt{T_\parallel}} e^{-mv_\perp^2/2T_\perp - mv_\parallel^2/2T_\parallel} 2\pi v_\perp dv_\perp dv_\parallel . \tag{5}$$

The friction force components can be accurately calculated using numerical evaluation of the integral in Eq. (1). However, asymptotic expressions based on the Coulomb analogy [9, 10] are frequently used instead, due to their simplicity. If the transverse rms velocity of the electrons $\Delta_\perp$ is substantially larger than the longitudinal velocity spread $\Delta_\parallel$, the friction force can be approximated in three ranges of the ion velocity, for example, as follows [9].

For high ion velocities, $v_i >> \Delta_\perp$, the longitudinal and transverse components of the friction force are equal:

$$\vec{F} = -\frac{4\pi Z^2 e^4 n_e L}{m} \cdot \frac{\vec{v}_i}{v^3}, \tag{6}$$

and, in this range, the friction force shape agrees asymptotically with Eq. (4). For ion velocities in the range $\Delta_\parallel << v_i << \Delta_\perp$, the friction force components are given by:

$$\vec{F}_\perp = -\frac{4\pi Z^2 e^4 n_e L}{m} \cdot \frac{v_{i,\perp}}{\Delta_\perp^3}, \qquad F_\parallel = -\frac{4\pi Z^2 e^4 n_e L}{m} \frac{v_\parallel}{|v_\parallel| \Delta_\perp^2}. \tag{7}$$

In the limit of very low ion velocities, $v_i << \Delta_\parallel$, the transverse component of the friction force is zero, and the longitudinal component is given by:

$$F_\parallel = -\frac{4\pi Z^2 e^4 n_e L}{m} \frac{v_\parallel}{\Delta_\parallel \Delta_\perp^2}. \tag{8}$$

The friction force based on the asymptotic expressions has been compared with direct numerical integration, based on Eq. (1), using the BETACOOL code. It was found that these asymptotic formulas can overestimate the friction force by a factor of two or higher, even for relatively large anisotropy of the electron distribution. Since our primary goal is to have an accurate description of the friction force, for comparison with VORPAL simulations, we prefer to use numerical integrals rather than the asymptotic expressions given above.

Figure 1 compares VORPAL data (dots with error bars) with the force described by Eq. (4) (blue solid line) and the result of numerical integrations based on Eq. (1) (red dashed line), for the case of an isotropic Maxwellian distribution of electrons, where $\Delta_\perp=\Delta_\parallel$=1.0e5 m/s (Z=79, n_e=2e15 m^{-3}). For all VORPAL simulations presented in this paper, the electron/electron interactions are neglected, which is valid for sufficiently short interaction times. The interaction between ions and electrons is limited by the time of flight through the cooling section, which is 4e-10 s in the PRF, for a cooling section length L=13 m and relativistic factor γ=108 for the Au^{+79} ions in RHIC. For typical parameters of the RHIC cooler, the interaction time is smaller than or comparable to the plasma period.

Since only very short interaction times are simulated with VORPAL, the rms spread in the ion velocity changes, due to diffusion, is significant and can be larger than the velocity reduction due to friction for a single pass. This makes it difficult to accurately extract the friction force from simulated ion velocities. Some special tricks are being employed to suppress the diffusive aspect of the ion dynamics [3], because our primary interest here is the friction force. For each VORPAL data point shown in the figures, corresponding to a single initial ion velocity, we have generated 100's of ion trajectories, $N_{traj.}$, and plotted the mean velocity drag (or, equivalently, the mean

friction force). According to the Central Limit Theorem, the uncertainty in these mean values is +/- 1 rms/$(N_{traj.})^{1/2}$, which is what we've used for the error bars.

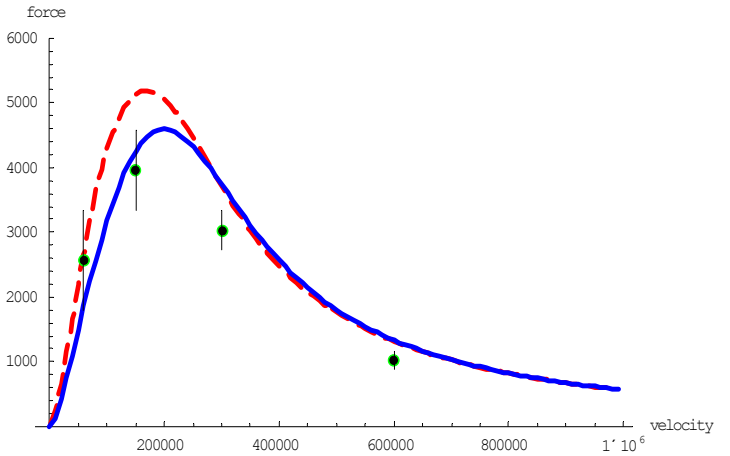

FIGURE 1. Non-magnetized friction force for an isotropic Maxwellian distribution of electron velocities with $\Delta_{\perp}=\Delta_{||}=1.0e5$ m/s. Force [eV/m] vs. ion velocity [m/s]: solid blue line – Eq. (4); dashed red line – numeric integration using BETACOOL; points with error bars –VORPAL simulations.

Figure 2 compares VORPAL data (dots with error bars) with the result of numerical integration based on Eq. (1) (solid red line), for the case of an anisotropic Maxwellian distribution of electrons, where $\Delta_{\perp}=4.2e5$ and $\Delta_{||}=1.0e5$ m/s (Z=79, $n_e=2e15$ m^{-3}).

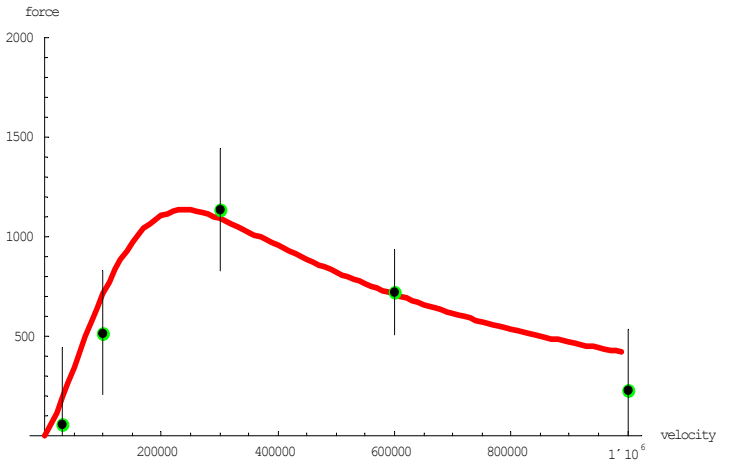

FIGURE 2. Non-magnetized friction force for an anisotropic electron distribution. Force [eV/m] vs. ion velocity [m/s]: solid line (red) – numeric integration using BETACOOL; points with errors bar – simulations using VORPAL.

Simulations were done for other degrees of anisotropy of electron velocity as well. We find agreement between VORPAL simulations and numeric integration satisfactory, and thus use the non-magnetized friction force in BETACOOL based on numerical integration in our dynamics studies of the non-magnetized cooling [4].

MAGNETIZED FRICTION FORCE

The presence of a strong longitudinal magnetic field changes the collision kinetics. The magnetic field limits transverse motion of the electrons. In the limit of very strong magnetic field, the transverse degree of freedom does not take part in the energy exchange, because collisions are adiabatically slow relative to the Larmor oscillations. As a result, the efficiency of electron cooling is determined only by the longitudinal velocity spread of electrons. In typical low-energy electrostatic coolers, the longitudinal velocity spread of electrons is much smaller than the transverse one. Thus an effect of strong velocity anisotropy together with the magnetic field leads to very fast magnetized cooling. In applications to higher-energy cooling, this advantage is somewhat limited due to the significant contribution to the effective velocity spread of electrons from the imperfections of the cooling solenoid. For example, for the RHIC cooler, assuming solenoid imperfections with an rms angle at the level of 1e-5, the effective angular spread in the beam frame is larger by the factor γ=108, or ~1e-3 m/s.

Since the friction force cannot be written analytically in closed form for arbitrary strength of the magnetic field, numerical simulations are required to explore in detail collisions between magnetized electrons and ions. In recent years, a lot of studies in this area were done by the Erlangen group [11]. However, to the best of our knowledge, a systematic comparison with the friction force formulas used by the electron cooling community have not been reported. In this paper, we attempt such a comparison with available formulas using the VORPAL code.

In the limit of a very strong magnetic field, where transverse motion of electrons is completely suppressed, the result for the magnetized friction force was written by Derbenev and Skrinksy in the following form [10]:

$$\vec{F} = \frac{2\pi Z^2 e^4 n_e}{m} \frac{\partial}{\partial \vec{V}} \int \left[\frac{V_\perp^2}{U^3} L_M + \frac{2}{U} \right] f(v_e) dv_e , \tag{9}$$

where Z is the ion charge number, e is the electron charge, n_e is the electron density, m is the electron mass, $\vec{V} = (V_\perp, V_\parallel)$ is the ion velocity, $U = \sqrt{V_\perp^2 + (V_\parallel - v_e)^2}$ is the relative velocity of the ion and an electron "Larmor circle," with transverse electron velocities being completely suppressed (i.e. approximation of infinite magnetic field). The actual values of the magnetic field and transverse rms electron velocity spread enter only via the cutoff parameters under the Coulomb logarithm, which is defined as

$$L_M = \ln\left(\frac{\rho_{\max}}{\rho_L} \right) \qquad \rho_L = \frac{cm\Delta_\perp}{eB} . \tag{10}$$

The function in Eq. (9) has asymptotes in the region of small and large ion velocities. When V >> $\Delta_\parallel$, the electron distribution can be approximated by the delta-function $f(v_e) = \delta(v_e)$, and integration of (9) gives [10]:

$$F_\parallel = -V_\parallel \frac{2\pi Z^2 e^4 n_e}{mV^3} \left(\frac{3V_\perp^2}{V^2} L_M + 2 \right), \tag{11}$$

$$F_\perp = -V_\perp \frac{2\pi Z^2 e^4 n_e L_M}{mV^3} \frac{V_\perp^2 - 2V_\parallel^2}{V^2} . \tag{12}$$

When the ion velocity is sufficiently less then electron velocity spread V << $\Delta_{\|}$, the friction force can be expressed as [10]:

$$F_{\|} \approx -2\sqrt{2\pi}\frac{Z^2 e^4 L_M}{m\Delta_{\|}^3} V_{\|}, \tag{13}$$

$$F_{\perp} \approx -2\sqrt{2\pi}\frac{Z^2 e^4 L_M}{m\Delta_{\|}^3} \ln\left(\frac{\Delta_{\|}}{V_{\perp}}\right) V_{\perp}. \tag{14}$$

We note that Eq. (9) and the asymptotic expressions in Eq.'s (11) and (12) were originally derived based on a perturbative treatment of the collective plasma response. It was later suggested by Parkhomchuk [12] that one gets slightly different asymptotic expressions using the binary collisions approach. Because the difference between these two approaches only slightly affects the final expression for the asymptotics given in Eq.'s (11) and (12), we leave this issue to future work.

As for the non-magnetized case, one can compare the accuracy of asymptotic expressions with numerical integration over the electron velocity distribution. Such numerical integration was recently implemented in the BETACOOL code, using Eq, (9), in the following form:

$$F_{\perp}\left(V_{\perp}, V_{\|}\right) = -\frac{2\pi Z^2 e^4 n_e L_M}{m}\int \frac{V_{\perp}\left(V_{\perp}^2 - 2\left(V_{\|} - v_e\right)^2\right)}{\left(V_{\perp}^2 + \left(V_{\|} - v_e\right)^2\right)^{5/2}} f\left(v_e\right) dv_e, \tag{15}$$

$$F_{\|}\left(V_{\perp}, V_{\|}\right) = -\frac{2\pi Z^2 e^4 n_e}{m}\int \left(L_M \frac{3V_{\perp}^2\left(V_{\|} - v_e\right)}{\left(V_{\perp}^2 + \left(V_{\|} - v_e\right)^2\right)^{5/2}} + 2\frac{V_{\|} - v_e}{\left(V_{\perp}^2 + \left(V_{\|} - v_e\right)^2\right)^{3/2}} \right) f\left(v_e\right) dv_e. \tag{16}$$

Recently, to account for finite values of the magnetic field, an empirical expression for the magnetized friction force was suggested by Parkhomchuk [13]:

$$\vec{F} = -\vec{v}\frac{4Z^2 e^4 n_e L_P}{m}\frac{1}{\left(v^2 + \Delta_{e,eff}^2\right)^{3/2}}, \tag{17}$$

where $\Delta_{e,eff}$ is the effective electron velocity spread. In the absence of space-charge effects, $\Delta_{e,eff}$ is the longitudinal velocity spread of electrons, with an additional contribution from the effective angles of variations in the magnetic field lines. The Coulomb logarithm in Eq. (17) is given by

$$L_P = \ln\left(\frac{\rho_{\max} + \rho_{\min} + \langle\rho_{\perp}\rangle}{\rho_{\min} + \langle\rho_{\perp}\rangle}\right). \tag{18}$$

Figure 3 shows the longitudinal friction force as a function of the longitudinal ion velocity, for the case of zero transverse ion velocity. The VORPAL simulations are done for the following parameters: B=5T, time of interaction in beam frame 0.4 ns, $\Delta_{\perp}$=1.1e7 and $\Delta_{\|}$=1.0e5 m/s, Z=79 and n_e=2e15 m^{-3}. One can see that the asymptotic expressions overestimate the friction force by a significant factor. The numerical integrations from BETACOOL show friction force values similar to the expression in Eq. (17), which compare well with VORPAL results but with the maximum shifted towards higher ion velocities. For the effective velocity in Eq. (17) we did not assume any contribution except for $\Delta_{\|}$=1.0e5 m/s. For ion motion along the magnetic field

lines, the expression in Eq. (17) is very close to the results of VORPAL, for the parameters mentioned above.

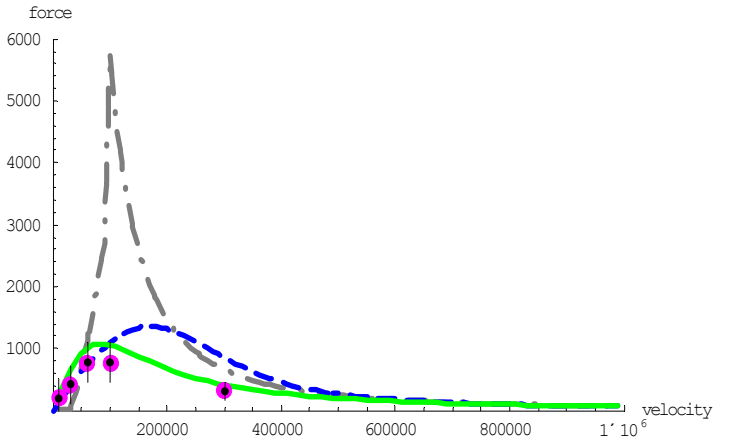

FIGURE 3. Magnetized friction force [eV/m] vs. longitudinal ion velocity [m/s]: solid line (green) – empiric formula by Parkhomchuk (Eq. 17); dot-dash line (gray) – Derbenev-Skrinksy-Meshkov asymptotic expressions [9]; dash line (blue) – Derbenev's expression with numerical integration over electron distribution (Eq. 16); dots with error bars – VORPAL results.

Figure 4 shows simulations using the same parameters as in Fig. 3, but with two different sets of transverse rms electron velocities: $\Delta_{\perp}$=1.1e7 m/s (pink, lower data set) and 4.2e5 m/s (red, upper data set), with good magnetized cooling seen in both cases. This difference in the transverse electron velocities results in a factor of 2.2 change in the magnetized Coulomb logarithm for fixed ion velocity. The corresponding change in the cooling force is reproduced by the VORPAL simulations and also by Eq. (17), which is plotted as green lines in Fig 4.

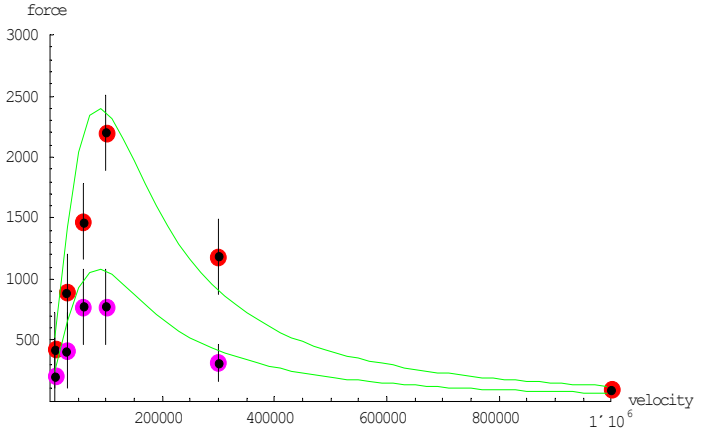

FIGURE 4. Magnetized friction force for ion velocities parallel to magnetic field lines. Force [eV/m] vs. longitudinal ion velocity [m/s]: upper curve (Eq. 17) and red dots (VORPAL data) for $\Delta_{\perp}$=4.2e5 m/s; lower curve (Eq. 17) and pink dots (VORPAL data) for $\Delta_{\perp}$=1.1e7 m/s.

Angular Dependence for Large Relative Velocities

An important feature of rigorous description in a strong magnetic field is that for relative velocities much higher than the longitudinal spread of electrons, the component of the friction force in the longitudinal and transverse directions have very different forms, as can be seen from Eq. (11) and (12). The first important feature is a specific dependence of the transverse angle between an ion velocity and the direction of the magnetic field line, which is plotted in Fig. 5 for the longitudinal component of the friction force. The solid blue line corresponds to Eq. (11).

In order to simulate the same behavior, we need to reproduce conditions similar to those assumed in the derivation of first Eq. (9) and then Eq. (11). This corresponds to zero rms electron velocities in both the transverse and longitudinal degrees of freedom. The lower cutoff parameter in the Coulomb logarithm of Eq. (9) is modeled, for such idealized "cold" case, with a 'cloud' or softening parameter introduced in the direct numerical simulations of the drag force. Figure 5 shows that, when such approximations are specifically introduced in the simulations, the agreement between simulations and Eq. (11) is very good.

However, this "cold-beam" approximation is far from valid in real situations. For example, the blue dots without error bars correspond to finite rms velocity spreads of the electron beam, as is expected for the case of magnetized cooling in RHIC, with $\Delta_{\perp}$=1.1e7 and $\Delta_{\parallel}$=1.0e5 m/s. The dependence on the angle between the ion velocity and the magnetic field lines, which is dramatic in the idealized cold case, is still seen, but it is now much less pronounced. In fact, the finite temperature results are not much different from the empirical formula in Eq. (17), which completely ignores any angular dependence with respect to the strong magnetic field. Similar arguments were made previously by Parkhomchuk [13].

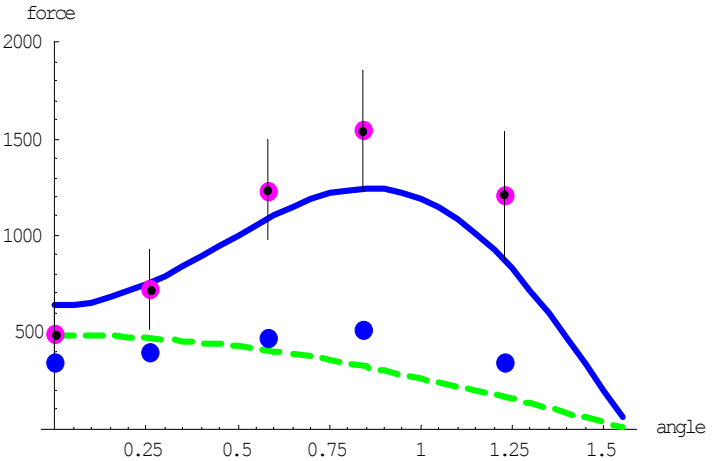

FIGURE 5. Dependence of the longitudinal component of the friction force on transverse angle with respect to magnetic field lines. Force [eV/m] vs. angle [rad]: solid blue line – Derbenev-Skrinsky asymptotics; dashed green line – VP empirical formula (Eq. 17); pink dots with errors bars – VORPAL simulations of ultra-cold electron beam; blue dots without errors bars – VORPAL simulations of finite temperature electrons.

For the transverse component of the friction force, VORPAL simulations show 'anti-friction' as predicted by the asymptotic formulas. This is shown for the case of cold electron beam simulations in Fig. 6. The detailed discussions of the amount of observed anti-friction, comparison with different approaches [10,12], and discussion for the finite temperature electron beam will be reported elsewhere.

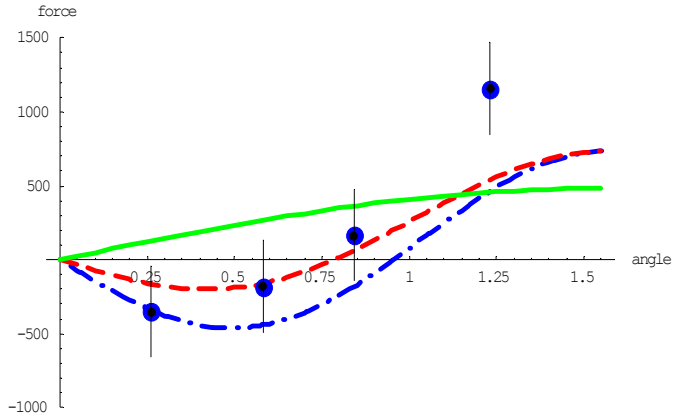

FIGURE 6. Dependence of the transverse component of the friction force on transverse angle. Force [eV/m] vs. angle [rad]: blue dot-dash line – Eq. (12) asymptotics based on the dielectric approach; red dashed line – asymptotics based on the binary collisions approach [12]; green solid line – empirical formula in Eq. (17); dots with errors bars – VORPAL simulation for ultra cold electron beam.

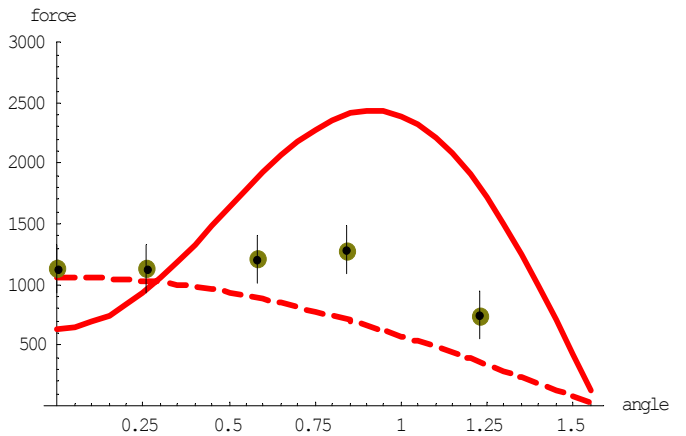

FIGURE 7. Dependence of the longitudinal component of the friction force on transverse angle with respect to magnetic field lines. Force [eV/m] vs. angle [rad]: red solid line – asymptotics in Eq. (11); red dashed line – Eq. (17); dots with errors bars – VORPAL simulations for $\Delta_{\perp}$=4.2e5 m/s.

Another important feature of Eq. (11) is the behavior at zero transverse angle (i.e. zero transverse ion velocities), which would lead to zero longitudinal friction force in the absence of a non-logarithmic term. However, the origin of this constant term in Eq. (11) has a completely different nature, and is due to phenomena which are not included in the present simulations. (Detailed discussion of these issues is beyond the scope of this paper.) As a result, this constant term has no dependence on the magnetized Coulomb logarithm and, in fact, should be zero in our simulations.

The appearance of finite values for the longitudinal friction force at zero transverse angle in our simulations is due to the fact that we allow for all possible exchanges of electron energy with ions during the finite time of interaction. Our simulations show scaling with the magnetized logarithm at zero transverse angle. This is shown in Fig. 7 for $\Delta_\perp$=4.2e5 m/s. The friction force is increased by the factor expected based on the magnetized logarithm, as compared to the case with $\Delta_\perp$=1.1e7 m/s, shown in Fig. 5. Such scaling with the magnetized logarithm at zero transverse angle is also in good agreement with Eq. (17), although that formula does not include the full dependence on the transverse angle, as can be seen for other values of angles plotted in Fig. 7.

SUMMARY

Direct numerical simulations of binary collisions with the VORPAL code have allowed us to explore the accuracy of various formulas and approximations, both for the non-magnetized and magnetized friction force. Using these simulations, we are in a position to explore detailed aspects of magnetized cooling, some of which are reported in this paper. For some simple cases, a comparison with numerical integration of the friction force expressions using the BETACOOL code have also been shown. These studies enable us to use appropriate friction force formulas with a known degree of accuracy, which is very important for future facilities that will depend on high-energy magnetized cooling.

ACKNOWLEDGMENTS

We are grateful for Ilan Ben-Zvi and Vladimir Litvinenko for many useful discussions and suggestions during these studies. We also thank A. Burov, Ya. Derbenev, and the Accelerator Physics Group of Electron Cooling Project of RHIC for constant support and stimulating discussions. The support and constant help of Tech-X Corp. with the VORPAL code and the Dubna Cooling group with the BETACOOL code is greatly appreciated. Work supported by the US Department of Energy.

REFERENCES

1. C. Nieter, J. Cary, J. Comp. Phys. **196** (2004) , p. 448.
2. RHIC E-cooler Design Report, http://www.agsrhichome.bnl.gov/eCool
3. D.L. Bruhwiler *et al*., AIP Conf. Proceed. **773** (Bensheim, Germany, 2004), p. 394.
4. A.V. Fedotov *et al*., Proceedings of PAC'05 (Knoxville, TN), TPAT089.
5. BETACOOL program , http://lepta.jinr.ru
6. S. Chandrasekhar, *Principles of Stellar Dynamics* (U. Chicago Press, 1942).
7. NRL Plasma Formulary, ed. J.D. Huba (2000).
8. G.I. Budker. At. Energy **22** (1967), p. 346.
9. I. Meshkov, Phys. Part. Nucl. **25** (1994) , p.631. (and references therein)
10. Ya. Derbenev, A. Skrinsky, Part. Acc. **8** (1978) , p. 235; Sov. Phys. Rev **1** (1981), p. 165.
11. C. Toepffer, Phys. Rev. A **66**, 022714 (2002); H.B. Nersisyan, G. Zwicknagel ands C. Toepffer, Phys. Rev. E **67**, 026411 (2003). (and references therein)
12. V. Parkhomchuk, "Physics of fast electron cooling," Electron Cooling Workshop (Karlsruhe, 1984).
13. V. Parkhomchuk, Nucl. Inst. Meth. A **441**, p. 9 (2000).